JOURNAL OF SOLID STATE CHEMISTRY 55, 92–100 (1984)

The Jahn–Teller Cooperative Effect in $Cu_{1-x}Zn_xSiF_6 \cdot 6H_2O$

B. YA. SUKHAREVSKII, F. A. BOIKO, A. M. BYKOV,
V. E. GANENKO, E. O. TSIBULSKII, AND G. E. SHATALOVA

Physico-Technical Institute, Academy of Sciences of the Ukr. SSR, 340114 Donetsk, USSR

Received October 1, 1982; in revised form June 1, 1984

The properties of $CuSiF_6 \cdot 6H_2O$ and $Cu_{0.9}Zn_{0.1}SiF_6 \cdot 6H_2O$ crystals were studied using X-Ray analysis and adiabatic calorimetry. The measurements cover the temperature range from 100 to 310 K. The enthalpy of transition for the phase transitions which occur at 300 K have been obtained and the crystal lattice parameters of the high-temperature phase of $Cu_{0.9}Zn_{0.1}SiF_6 \cdot 6H_2O$ have been determined. These results furnish additional proof for the assumption that this transition involves the cooperative Jahn–Teller effect. The partial dehydration of specimens with loss of two water molecules in the phase-transition region, and the anomalous temperature dependence of the lattice parameters can be explained by stability loss of the initial phase over the pretransitional temperature range.

1. Introduction

As is known, an instability of the initial phase in the vicinity of the second-order phase transition is frequently observed. A similar phenomenon may be supposed to take place for certain nondiffusional first-order phase transition. In the present paper an attempt is made to show that such structural instabilities are revealed at the first-order phase transitions, due to the cooperative Jahn–Teller effect. Such a possibility arises from the fact that the Jahn–Teller cooperative effect leads to both first-order and second-order phase transitions; in the latter case such an instability is well documented (*1*). A knowledge of the microscopic mechanism leading to the change of structure at a phase transition is of considerable assistance in interpreting experimental results.

The hexahydrate of copper fluorsilicate $CuSiF_6 \cdot 6H_2O$ is taken as the object of the present study. The structure of this crystal at room temperature has been determined in (*2*). It consists of two types of columns, both made up by alternate stacking of $Cu(H_2O)_6^{2+}$ and SiF_6^{2-} octahedra along the direction of the threefold axis. While the SiF_6 octahedra are regular in both types of columns, $Cu(H_2O)_6^{2+}$ octahedra are regular in one (one-fourth of copper atoms) and triclinically distorted in other (three-fourths of copper atoms). The temperature dependence of the heat capacity (*3*) and the magnetic anisotropy (*4*) at the first-order phase transition at temperature 295 K in this substance is generally interpreted in terms of the cooperative Jahn–Teller effect. This interpretation is supported by the static (at lower temperatures) and dynamic Jahn–Teller effect in $Cu(H_2O)_6^{2+}$ complexes, in a

0022-4596/84 $3.00

diamagnetic matrix $ZnSiF_6 \cdot 6H_2O$ (*5*), and also, by the similarity of the first coordination sphere of the Cu^{2+} ion in $CuSiF_6 \cdot H_2O$ and in potassium, cesium, and thallium cuprates, for which the Jahn–Teller effect has already been demonstrated (*6–8*). However, in these cuprates the high-temperature phase is of cubic symmetry, and in the low-temperature phases the $Cu(NO_2)_6^{2+}$ complexes are tetragonally distorted. The $CuSiF_6 \cdot 6H_2O$ crystals have nonorthogonal symmetry (their symmetry is described by the space group $R\bar{3}$), while $Cu(H_2O)_6^{2+}$ complexes at low temperatures exhibit triclinic distortions (*2*), which is of great interest. The effect of diamagnetic impurities on the phase transition in $CuSiF_6 \cdot 6H_2O$ have been studied by means of a partial substitution of ions Cu^{2+} with diamagnetic ions Zn^{2+}.

2. Specimen Preparation

To prepare specimens $CuSiF_6 \cdot 4H_2O$ and $ZnSiF_6 \cdot 6H_2O$ starting materials of 98.65 and 99.8%, respectively, were used. Cu $SiF_6 \cdot 6H_2O$ was prepared by crystallization from an aqueous solution at 14,00(5)°C (*4*). The necessary supersaturation was attained by slow vaporization of water. The resulting transparent blue crystals were regular in shape and had linear dimensions ranging from 5 to 10 mm. The solid solutions $Cu_{1-x}Zn_xF_6 \cdot 6H_2O$ were prepared in the same manner from aqueous solutions of $CuSiF_6 \cdot 6H_2O$ and $ZnSiF_6 \cdot 6H_2O$, the concentration of the latter being 3%. A chemical analysis of the crystals was carried out using the atom-adsorption method; this showed that $x = 0.1$. The x-values in crystals depend on the crystallization temperature and on the $ZnSiF_6 \cdot 6H_2O$ content in the solution. Therefore, to prepare homogeneous specimens, great care was taken to maintain temperature stability and to achieve the concentration of the initial solution. The absence of tetrahydrate in the final specimens was checked by using chemical titration and X-Ray analysis.

3. X-Ray Studies

X-Ray studies were carried out by powder X-Ray analysis with a diffractometer DRON-2. The thermostat URNT-180 was used to maintain temperature in the range 90–320 K, with less than a 0.4 K deviation during the time of the experiment. The crystals were pulverized at 10°C, precautions being taken to avoid dehydration. A small quantity (a few percent) of the salt solution was retained in the sample.

The diffractograms of $CuSiF_6 \cdot 6H_2O$ and $Cu_{0.9}Zn_{0.1}SiF_6 \cdot 6H_2O$ in the temperature range 280–290 K (phase II) are completely indexed in the space group $R\bar{3}$, a = 18.138(2) Å, c = 9.878(5) Å, Z = 12, and a = 18.200(2) Å, c = 9.836(5) Å, Z = 12, respectively. This is in good agreement with the results of other structural studies (*2*). On heating $Cu_{0.9}Zn_{0.1}$ $SiF_6 \cdot 6H_2O$ crystals undergo a phase transition in the temperature range from 296 to 302 K. The atomic structure of the high-temperature phase (phase I) of $Cu_{0.9}Zn_{0.1}SiF_6 \cdot 6H_2O$ was determined by optimizing the comparison between experimental and calculated intensities, using the program "Polycrystal" (*9*). The inaccuracy factor value of R = 0.11 was obtained. The symmetry of phase I is described by the space group $R\bar{3}$; the lattice parameters are a = 9.344(2) Å, c = 9.695(5) Å, Z = 3. The structure is formed by two similar sublattices of regular octahedra $Cu(H_2O)_6^{2+}$ and SiF_6^{2-}. In the positions of the SiF_6^{2-} complexes octahedra of two types (in relation 0.4/0.6) are statistically distributed, differing by angles of rotation relative to the $Cu(H_2O)_6^{2+}$ octahedra. The interatomic distance Cu–O equals 2.19(3) Å. Thus, at the transition I → II, three-fourths of octahedra are distorted, and the period a of a hexagonal unit is doubled. No transition to phase I was observed

TABLE I

INTEGRATED INTENSITIES OF X-RAY REFLECTIONS AND CORRESPONDING CONCENTRATIONS OF PHASES I AND II AS WELL AS THEIR TETRAHYDRATE MODIFICATION FOR THE SAMPLE OF $Cu_{0.9}Zn_{0.1}SiF_6 \cdot H_2O$ AT DIFFERENT TEMPERATURES

		Integrated intensity impulse per sec			Phase concentrations, vol%			
Cycles	T K	Phase I	Phase II	Tetrahydrate modification	Phase I	Phase II	Tetrahydrate modification	Sum of phase concentrations
Heating	290.0	58,800	206,000	145,300	0	0.912	0.084	0.996
	300.5	105,604	58,800	285,456	0.668	0	0.321	0.989
Cooling	292.0	90,500	100,436	266,000	0.458	0.258	0.288	1.004
	287.5	87,691	112,000	270,500	0.415	0.322	0.295	1.032
	282.5	85,300	116,700	272,600	0.379	0.351	0.299	1.029
	273.0	80,700	12,130	273,407	0.311	0.380	0.300	0.990

in case of $CuSiF_6 \cdot 6H_2O$ due to formation in the above temperature region of the tetrahydrate in large quantities.

Figure 1 shows the temperature dependence of the intensities of (242) lines for phase II and of (122) lines for phase I for $Cu_{0.9}Zn_{0.1}$ $SiF_6 \cdot 6H_2O$ sample during heating and cooling by 1.5 K steps of 8 min duration. The intensities are specified in terms of the initial intensity of the (242) line for phase II, the measurement error being 3%. The transition II → I takes place in the temperature range 295–303 K and is accompanied by hysteresis. The phase transition

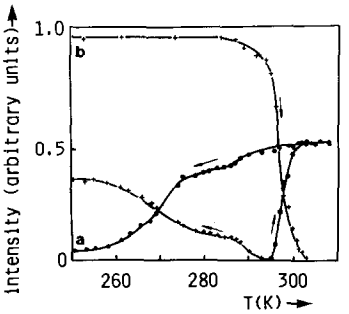

FIG. 1. Temperature dependence of line intensity in the diffractograms of $Cu_{0.9}Zn_{0.1}SiF_6 \cdot 6H_2O$. (a) lines (122) of phase I, (b) lines (242) of phase II. Intensities are normalized with respect to the initial intensity of line (242) of phase II; arrows indicate the direction of temperature change.

for the cooling cycle is more extended. The line intensities of phase II after the phase transition is completed are substantially lower than the initial ones. This is associated with the appearance of the tetrahydrate whose formation takes place simultaneously with the phase transition.

Quantitative estimates for the correlation of phases are provided in Table I. The calculations were based on the assumption that the phase concentrations are proportional to the integrated line intensities for corresponding phases after subtraction of the background. At every temperature, the intensity of phase lines was determined with some delay, to allow for establishment of a uniform concentration.

The temperature dependence for the integrated intensity of the (111) peak for the $CuSiF_6 \cdot 4H_2O$[1] formed in hexahydrate in the region of phase transitions II → I, is shown in Fig. 2. A reduction of this line intensity with decreasing temperature, observed at phase transition I → II, indicates a partial reduction of the hexahydrate, due to a decrease in the amount of tetrahydrate. A comparison of Figs. 2 and 1 shows that the largest amount of tetrahydrate is

[1] The absence of phase transitions in $CuSiF_6 \cdot 4H_2O$ was established by special experiments.

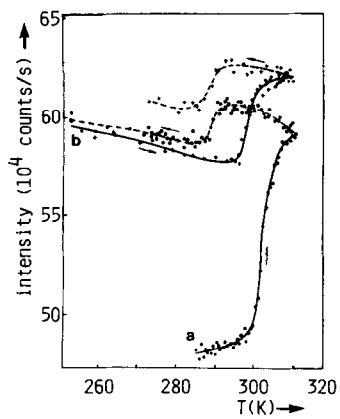

FIG. 2. Temperature dependence of the integral intensity of line (III) of tetrahydrate in the vicinity of the I → II phase-transition temperatures for $Cu_{0.9}Zn_{0.1}SiF_6 \cdot 6H_2O$. (a) First heating–cooling cycle, (b) second heating–cooling cycle.

formed in the temperature range of the phase transition II → I.

The amount of tetrahydrate formed during phase transition II → I increases with decreasing crystal size. Thus, for $Cu_{1-x}Zn_xSiF_6 \cdot 6H_2O$ monocrystals the amount of tetrahydrate is at least 10 times less than for powders with crystal sizes $\sim 10^{-3}$. For a given size of crystals, the quantity of tetrahydrate decreases with diminishing Zn^{2+} concentration. During the study of finely dispersed powders ($\sim 10^{-3}$ cm) at temperatures above the transition point, the $CuSiF_6 \cdot 6H_2O$ sample transforms practically completely to the tetrahydrate.

The ratio of phases present at any given temperature depends also on the delay time. The curves in Fig. 3 exhibit the character of isothermal kinetics of the phase transitions II → I and I → II. The formation of tetrahydrate at constant temperature in the region of transition II → I, and its decrease at the start of transition I → II also continues with time. The maximum rate of these processes is reached at temperatures near the start of the phase transitions.

The temperature dependence of crystal lattice parameters $a/2$ and c, and of the volume v corresponding to one formula unit for $CuSiF_6 \cdot 6H_2O$ and $Cu_{0.9}Zn_{0.1}SiF_6 \cdot 6H_2O$ in phase II, is presented in Fig. 4. Of particular interest is the surprisingly high coefficient of thermal expansion (of the or-

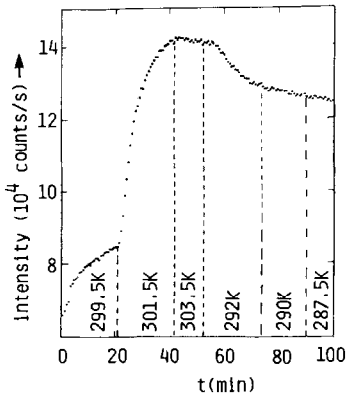

FIG. 3. Isothermic kinetics of phase transitions I ⇄ II in $Cu_{0.9}Zn_{0.1}SiF_6 \cdot 6H_2O$ based on the behavior of line (242) of phase I.

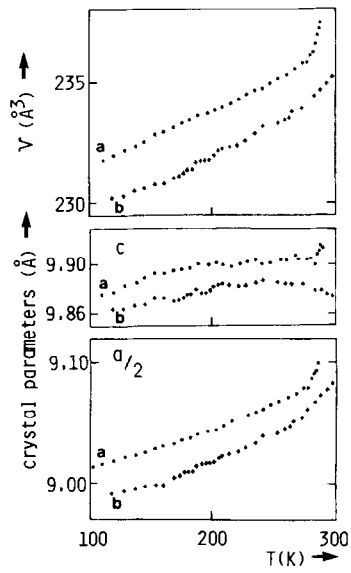

FIG. 4. Temperature dependence of volume v change corresponding to one formula unit and crystalline lattice parameters $a/2$ and c on heating of phase II. (a) $Cu_{0.9}Zn_{0.1}SiF_6 \cdot 6H_2O$; (b) $CuSiF_6 \cdot 6H_2O$.

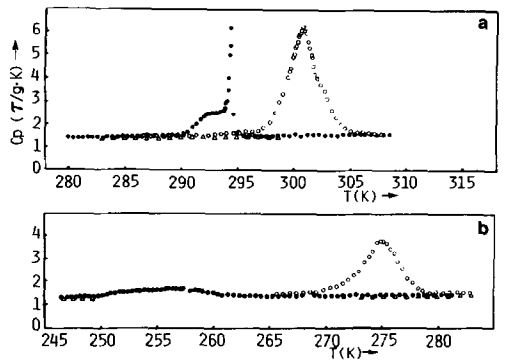

FIG. 5. Temperature dependence of heat capacity $Cu_{0.9}Zn_{0.1}SiF_6 \cdot 6H_2O$ (a) In the vicinity of phase transitions II → I; (b) in the vicinity of phase transitions at 275 K. (○) Heating, (●) cooling, (△) impulse regime.

der 10^{-4} cm^{-1}) along the *a* axis and its negative value along the *c* axis, when the phase transition temperature is approached. Beginning at 268 K, the system of X-Ray lines of phase II undergoes significant changes if cooling is conducted at very low rates (0.2 K/min). The cause of this, it seems, is one more transformation, which now is under study.

4. Calorimetric Studies

Calorimetric studies were carried out by continuous heating and cooling under nearly adiabatic conditions (the thermogram technique). The vacuum calorimeter with an automatic system for maintaining adiabatic conditions was previously described (*10*). $Cu_{0.9}Zn_{0.1}SiF_6 \cdot 6H_2O$ crystals with linear dimensions of 3 cm and a mass of 8.882 g were used in these measurements. Heating and cooling rates in different cycles varied from 0.05 to 0.15 K/min. Typical temperature variations of the heat capacity based on these thermograms are presented in Fig. 5. Thermal effects for a cooling cycle are represented, for convenience, as positive maxima. As can be seen, values obtained by continuous variation do not differ more than 3% from the heat capacity values obtained by the impulse technique. The error of the heat capacity measurements in the impulse method is ca. 0.2%; the accuracy of measurements in the continuous heating regime is substantially lower. However, what is highly important is that the thermogram technique allows one to obtain results not only on heating but also, on cooling. Thus, the analysis of eight cycles of heating–cooling showed that for the $Cu_{0.9}Zn_{0.1}SiF_6 \cdot 6H_2O$ sample the heat capacity maximum for the transition II → I occurs at 300.7(2) K on heating and at 294.9(5) K on cooling. For transformations at lower temperatures, the position of the maxima for heating and cooling are at 275.1(I) and ca. 257 K, respectively. Using the heating thermograms, the values of thermal effects associated with phase transitions have also been calculated. Unfortunately, it was impossible to obtain reliable quantitative estimates of thermal effects on cooling. Due to uncertainties in thermal flow values which could not be estimated directly in a cooling run, these values were chosen so as to force a coincidence of heat capacities in the cooling and heating cycles above the background.

From the calorimetric and X-ray studies it is reasonable to assume that the enthalpy ΔH_i for the transition II → I (in the *i*th heating-cooling cycle) should be specified as the heat of this transition and the heat of tetrahydrate formation:

$$\Delta H_i = \{M - m_i^h - m_{i-1}^I - \sum_{i=1}^{i-1} (m_i^h - m_i^c)\}h_1 + m_i^h h_2 \quad (1)$$

Here M is the initial mass of the sample, M_i^h is the mass of tetrahydrate formed on heating in the *i*th cycle, m_i^I is the mass of phase I retained in the sample after the completion of the *i*th cycle, h_1 is the heat of transition II → I, and h_2 is the heat of tetrahydrate formation.

The X-Ray studies of samples after com-

TABLE II

THE ENTHALPY AND CALCULATED THERMAL EFFECT OF DEHYDRATION FOR SOME HYDRATED COPPER SALTS

Complex	τ_T° (kJ/mole)	Reference	ΔH_T°, kJ/2 mole H_2O	
			Condensed water formed	Molecular-sorbe water formed
$CuCl_2 \cdot 4H_2O$	−1400	((*11*), p. 86)	19.7	86.7
$CuCl_2$	−216	((*12*), p. 118)		
$CuSO_4 \cdot 5H_2O$	−2278	((*12*), p. 130)	22.6	89.6
$CuSO_4 \cdot 3H_2O$	−1686	((*12*), p. 130)		
$CuBr_2 \cdot 4H_2O$	−1327	((*12*), p. 124)	20.1	87.1
$CuBr_2$	−143	((*12*), p. 122)		

pleting the calorimetric studies showed that six cycles of heating–cooling produced 0.1 *M* of tetrahydrate, so $m_i^I \approx 0.15$ *M* in every cycle. From the X-ray studies one finds that $m_i^c \approx 0.25\, m_i^h$, based on the assumption that tetrahydrate in the sample used in calorimetric studies accumulated in equal amounts during every cycle.[2] Thus it was assumed that $m_i^h - m_i^c \approx 0.017$ *M*; hence $m_i^h \approx 0.023$ *M*.

Since no data exist on the heat of dehydration of $CuSiF_6 \cdot 6H_2O$ (h_2) these values were estimated using thermochemical data (*11, 12*), tabulated for other complex compounds of copper.

Assuming that the energy values of chemical bond Cu–O are approximately the same for all hydrated copper salts, in which the Cu ion is in the octahedral coordination, the thermal effect of separation of two water molecules may be estimated according to the reactions

$$\tfrac{1}{2}CuCl_2 \cdot 4H_2O = \tfrac{1}{2}CuCl_2 + 2H_2O \quad (2)$$

$$CuSO_4 \cdot 5H_2O = CuSO_4 \cdot 3H_2O + 2H_2O \quad (3)$$

[2] As shown in several experiments, the selection of any smooth function to represent the tetrahydrate accumulation does not greatly affect the final result which remains the same within the intrinsic accuracy of the measurement.

$$\tfrac{1}{2}CuBr_2 \cdot 4H_2O = \tfrac{1}{2}CuBr_2 + 2H_2O \quad (4)$$

and from the equation

$$\Delta H_T^\circ = \Sigma \nu \tau_T^\circ \quad (5)$$

where ΔH_T° is the heat of reaction per 1 mole, τ_T° is the enthalpy of all reagents in their respective physical state (these values for salts are presented in Table II), and ν is the stoichiometric factor.

During the formation of the liquid phase the water molecules must diffuse through the crystalline lattice to the surfaces of macroscopic defects (pores, crystal boundaries, cracks). Since every heating–cooling cycle is restricted in time, at least part of water is maintained as an interstitial solid solution, i.e., kept in the lattice of the dehydrated crystal in the "molecular-sorbed" state by van der Waals forces. Therefore, in addition to the enthalpy for water in the condensed state, $\tau_{H_2O}^\circ = -286$ kJ/mole ((*11*), p. 110), the enthalpy value for water in molecular-sorbed state must be known. This is obtained from the vapor total enthalpy value (−242 kJ/mole) ((*11*), p. 109), corrected by the van der Waals bond value (−10.5 kJ/mole) (*13*), resulting in a value of −252 kJ/mole. The energy needed for the separation of two H_2O molecules lies in the range 21–88 kJ/mole (see also Table II).

Thus the heat of dehydration reaction

$$CuSiF_6 \cdot 6H_2O = CuSiF_6 \cdot 4H_2O + 2H_2O \quad (6)$$

lies in the range $70 < h_1 < 280$ J/g, depending on the ratio of water present in the condensed and molecular-sorbed state. The calculation using Eq. (1) shows that the heat of transition II → I is $7.8 < h_1 < 13.3$ J/g, and the entropy of this transition is $8.1 < \Delta S < 14$ J/mole · K.

Earlier estimates (*3*) do not agree with our results; as is now evident, large amounts of tetrahydrate in the sample had not been taken into account, as we did not control the state of phases.

5. Discussion

Comparison of structures of phases I and II shows that the regular $Cu(H_2O_6^{2+}$ octahedra of phase I (Fig. 6a) become distorted in passing to phase II. Unlike crystals with orthogonal symmetry, the distortions of $Cu(H_2O)_6^{2+}$ octahedra tend to be triclinic, though the structure does not deviate greatly from tetragonal (Fig. 6b). This seems to be connected with the nonorthogonality of the crystal structure. The stretching of one octahedron, coupled with a simultaneous reduction of two others, is characteristic of the Jahn–Teller effect in copper ions. The structural peculiarity of phase II, together with the data (*5–8*) mentioned in the Introduction confirms the assumption that the phase transition I → II is associated with a cooperative Jahn–Teller effect.

One may estimate the configurational entropy change at the phase transition II → I using the above reasoning concerning the nature of this transition. It is reasonable to assume that in phase I there will be uncorrelated distortions of the $Cu(H_2O)_6^{2+}$ octahedra of the same symmetry as in phase II. If the distorted octahedra in phase I are represented in equal measure by states which differ in their own and in induced rotation by an angle of 120°, then, on the average, they have the space symmetry $\bar{3}$ with respect to time or to lattice sites.

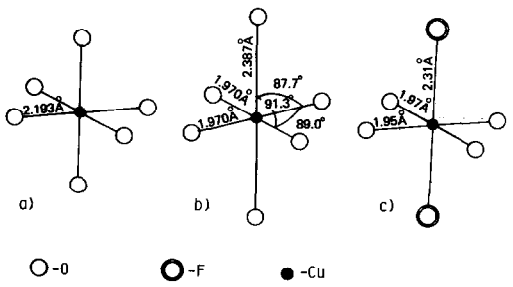

FIG. 6. The structure of octahedral complexes. (a) Perfect octahedron of phase I, (b) distorted octahedron of phase II, (c) octahedron in tetrahydrate of copper fluorosilicate.

Taking account of the fact that in phase II three-fourths of octahedra are distorted, the change of the configurational entropy at transition II → I for 1 mole may be written as

$$\Delta S_k = k_B \ln (\tfrac{3}{4})! \left[\left(\frac{3}{4}\frac{N}{6}\right)!\right]^{-6} = \tfrac{3}{4}R \ln 6 = 11{,}2\ \tau \cdot \text{mole}^{-1} \cdot K^{-1} \quad (7)$$

Here k_B is the Boltzmann constant, N is the Avogadro constant, $R = k_B N$ is the universal gas constant. Estimates of configurational entropy change for $Cu_{1-x}Zn_xSiF_6 \cdot 6H_2O$ are easily obtained by considering some limiting cases:

(1) the $Zn(H_2O)_6^{2+}$ octahedra are distorted due to the influence of the lattice as are the $Cu(H_2O)_6^{2+}$ octahedra; (2) the $Zn(H_2O)_6^{2+}$ octahedra are not distorted. This yields a range $10.1 < \Delta S_k < 11.2$ J/mole · K, but the experimental value falls in the range of $8.1 < \Delta S < 14$ J/mole.

The entropy jump at the phase transition is given by the sum of configurational and librational entropy changes. Since the temperature dependence of heat capacities of phases II and I, extrapolated to the transi-

tion temperature (Fig. 5a) (the weak temperature dependence of the heat capacities in the region of interest facilitates the extrapolation) is smooth at the junction point, the difference of the phonon spectra of phases I and II does not affect the integrated characteristics of these spectra. Thus, a comparison of the entropy jump found experimentally with the calculated value of configurational entropy change, is justified. The limiting estimated values of the entropy jump ΔS correspond to condensed and the molecular-sorbed states of water formed in the temperature range of the transition II → I. Since the calculated value of the entropy jump ΔS_k is within the range of estimated values of ΔS obtained from experiments, it may be concluded that water is present in both of the above-mentioned states. During the I → II phase transition, the molecules in the molecular-sorbed state may add to the tetrahydrate molecules to form the hexahydrate of phase II. This process is energetically favored since in the phase transition I → II the volume is decreased by 3%, whereas, at the tetrahydrate formation, it is increased by 25% thus compensating for elastic strains in the sample. Undoubtedly, this transformation is only partially realized, depending on the amount of H_2O retained in the molecular-sorbed state. As a result, the phase transition I → II extends over a greater range (Figs. 1, 5a). The same considerations apply to the phase transition II → I. They explain the connection between the temperature-dependent amounts of tetrahydrate and of $Cu_{0.9}Zn_{0.1}SiF_6 \cdot 6H_2O$ in phase I.

However, the tetrahydrate formation near the phase-transition temperature seem to be a direct consequence of the initial phase instability. Actually, a comparison of coordination octahedra of a Cu^{2+} ion in structures $CuSiF_6 \cdot 4H_2O$ (*14, 15*) (Fig. 6c) and phase II shows that tetrahydrate formation is accompanied by the loss of the two H_2O molecules most distant from a Cu^{2+} ion of the hexahydrate. This process occurs at a maximum rate in the temperature range of the cooperative Jahn–Teller effect, when H_2O molecules are extensively shifted from their equilibrium states in phase II.

This is confirmed to a certain extent by the anomalous temperature dependence of crystalline lattice parameters and by the volume of the elementary unit of phase II in the vicinity of phase transition II → I (Fig. 4). While still in the region of phase II 10 K away from the transition temperature these characteristics begin to change abruptly and to approach the value of corresponding characteristics of phase I. The change in lattice parameters terminates with a jump characteristic of the first-order transition. Nevertheless, it would be incorrect to consider such a phase transition as a first-order transition very similar to a second-order one, since it is characterized by high transition heat values (3 kJ/mole), by a volume discontinuity of 3%, and by substantial hysteresis.

Acknowledgment

The authors are grateful to Professor N. L. Yarym'-Agaev for useful advice.

References

1. G. A. Gehring, and K. A. Gehring, *Rep. Progr. Phys.* **38,** 1 (1975).
2. S. Ray, A. Zalkin, and D. H. Templeton, *Acta Crystallogr. Sect. B* **29,** 2748 (1973).
3. A. M. Bykov, V. E. Ganenko, V. I. Markovich, F. A. Steingart, and G. A. Tsintsadze, *J. Chem. Thermodyn.* **11,** 1065 (1979).
4. B. D. Bhattacharyya and S. K. Datta, *Indian J. Phys.* **42,** 181 (1968).
5. B. Bleaney and D. J. E. Ingram, *Proc. Phys. Soc. London Sect. A* **63,** 408 (1950).
6. Y. Noda, M. Mori, and Y. Yamada, *Solid State Commun.* **23,** 247 (1977).
7. M. Mori, N. Noda, and Y. Yamada, *Solid State Commun.* **27,** 735 (1978).
8. D. V. Harrowfield, A. J. Dempster, T. E.

FREEMAN, AND J. R. PILBROW, *J. Phys. C* **6**, 2058 (1973).

9. YU. G. TITOV, LERKHOROBIN, AND N. N. MATYUCHTSENKO, *Kristallografiya* **17**, 1053 (1972).
10. A. M. BYKOV, V. E. GANENKO, B. YA. SUKHAREVSKII, AND F. A. STEINGART, "Teployemkost' i termodinamicheskie svoistva geksagidrata ftorosilikata nikelya." Manuscript deposited in VINITI No. 3833-78 (1978).
11. M. KH. KARAPETYANTS AND M. P. KARAPETYANTS, "Osnovnye termodinamicheskie konstanty neorganicheskikh i organicheskikh vetschestv," Khimiya, Moskva (1968).
12. "Termodinamicheskie konstanty vetschestv" (V. P. Glushkov, Ed.), Vyp. 6, chast'I, VINITI, Moskva (1972).
13. W. KITTEL, "Vvedenie v fiziku tverdogo tela," 4 izd., Nauka, Moskva (1978).
14. J. FISHER, A. DE CIAN, AND R. WEISS, *Bull. Soc. Chim. Fr.* **8**, 2646 (1966).
15. M. J. R. CLARK, J. E. FLEMING, AND H. LINTON, *Canad. J. Phys.* **47**, 3859 (1966).